Crystal-field and magnetic properties of the distorted perovskite $NdGaO_3$

1993 J. Phys.: Condens. Matter 5 8973

(http://iopscience.iop.org/0953-8984/5/48/008)

J. Phys.: Condens. Matter 5 (1993) 8973–8982. Printed in the UK

Crystal-field and magnetic properties of the distorted perovskite $NdGaO_3$

A Podlesnyak†‡, S Rosenkranz†, F Fauth†, W Marti†, A Furrer†, A Mirmelstein‡ and H J Scheel§

† Laboratory for Neutron Scattering, ETH Zürich, and Paul Scherrer Institute, CH-5232 Villigen PSI, Switzerland

‡ Institute for Metal Physics, Russian Academy of Sciences, Yekateringburg GSP-170, Russia

§ Crystal Growth Group, Institute of Micro- and Optoelectronics, EPF Lausanne, CH-1007 Lausanne, Switzerland

Received 24 May 1993, in final form 13 August 1993

Abstract. Inelastic neutron scattering and magnetic susceptibility measurements have been performed on the distorted perovskite $NdGaO_3$. The magnetic susceptibility data show a Curie–Weiss behaviour with an effective magnetic moment close to $3.6\mu_B$ per mole of Nd ions. No long-range magnetic ordering was detected in the temperature range 2–300 K. The inelastic neutron spectra observed at $T = 12$ K exhibit four peaks of magnetic origin between 11 and 70 meV which can be unambiguously assigned to the complete crystalline-electric-field splitting pattern in the ground-state J multiplet $^4I_{9/2}$ of the Nd^{3+} ions. We analysed the spectra in terms of geometrical considerations based on the actual C_2 site symmetry of Nd^{3+}. The best agreement between the experimental spectra and the calculated level structure was obtained for a model that takes into account the three nearest-neighbouring coordination polyhedra associated with the O^{2-}, Ga^{3+} and Nd^{3+} ions as well as J-mixing between all multiplets of the ^4I term. We conclude that single-particle crystal-field theory adequately explains the majority of magnetic and crystal-field properties of $NdGaO_3$.

1. Introduction

The discovery of high-temperature superconductivity in layered perovskite systems [1] has generated considerable effort in the understanding of the physical properties of oxides having the perovskite and related structures. High-T_c compounds are close to the metal–insulator (MI) transition which occurs under decreasing oxygen content as well as under disordering. The parent compounds of copper-oxide superconductors are charge-transfer (CT) insulators (see, for example, [2]). Doping with extra holes or electrons turns these systems from the insulating regime into a metallic or superconducting regime. A few perovskite-type oxides are known to exhibit MI transitions. In most cases their mechanism is not yet well understood. Representatives of these systems are the ternary rare-earth–transition-metal–oxygen compounds. Recently synthesized distorted perovskites $RNiO_3$ (R=rare earth) exhibit a series of interesting properties, including a MI transition which is accompanied by significant changes of Ni–O–Ni angles and Ni–O distances [3], as well as by long-range magnetic ordering associated with the Ni sites [4]. The nature of the energy gaps in the nickelates is not yet understood. Thus, as pointed out in a recent article by Medarde *et al* [5] three kinds of gaps could be responsible for the MI transition in $RNiO_3$: Mott–Hubbard-type, CT-type, or negative-Δ-type, although a CT gap opening appears the most likely mechanism to explain the electronic localization.

0953-8984/93/488973+10$07.50

An interesting behaviour is also observed in the group of rare-earth aluminates, such as $PrAlO_3$ and $NdAlO_3$, which have $R\bar{3}2/c$ symmetry at room temperature and undergo a trigonal-to-cubic perovskite transition at high temperature [6]. Whereas $PrAlO_3$ has two additional phase transitions below room temperature, which are attributed to an interaction between the crystal vibrations and the electronic excitations of the Pr^{3+} ion [7], $NdAlO_3$ does not have any magnetic or structural transition down to $T = 2$ K.

$NdGaO_3$ is structurally related to the $RNiO_3$ and $RAlO_3$ compounds. However, there is no indication of any phase transition in the temperature region $2 < T < 300$ K. Therefore an investigation of the electronic structure of this compound is a good starting point for understanding the nature of structural transitions in aluminates, as well as the origin of magnetism and band gaps in nickelates. Inelastic neutron scattering (INS) is one of the most powerful techniques to investigate crystalline-electric-field (CEF) phenomena, particularly for optically opaque materials like the perovskite-type compounds, as extensively demonstrated in the past (see, for example, [8–10]). Moreover, CEF investigations for high-T_c superconductors provided direct evidence for CT processes [11] and phase separation [12].

In this paper we report results from INS and magnetic susceptibility measurements for $NdGaO_3$. From a fundamental point of view $NdGaO_3$ provides a good opportunity to study CEF effects in a low-symmetry environment, yielding significant contributions to the CEF Hamiltonian from both imaginary and odd terms. From the application point of view $RGaO_3$ compounds have considerable potential as a substrate material for high-temperature superconducting films, since their lattice and thermal-expansion behaviour is close to the 1–2–3 systems [13].

2. Experimental details

A single crystal of $NdGaO_3$ was grown by Czochralski pulling from a stoichiometric melt prepared from 99.99% Ga_2O_3 and Nd_2O_3. A non-oriented narrow $NdGaO_3$ crystal from an earlier growth experiment was used as a seed. The pull and rotation rates were successively changed from an initial 2.5 mm h^{-1} and 30 rpm for the seeding phase to 1.3 mm h^{-1} and 20 rpm during growth of the crystal cylinder of 25.4 mm diameter and 63 mm length. After a total of 64 hours growth the 317 g crystal was programme-cooled to room temperature. The dark crystal with typical Nd absorption was free from macroscopic inclusions, and nearly free from cracks and twin boundaries. Part of the crystal was used for the preparation of the polycrystalline material.

The magnetic susceptibility was measured on a single crystal (0.23 g) by the Faraday balance technique in a magnetic field of 0.004 T at temperatures ranging from 5 to 300 K. The magnetization on a powder sample was measured with a superconducting-quantum-interference-device (SQUID) magnetometer [14] in the temperature range 2–300 K.

The neutron scattering experiments were performed at the Saphir reactor in Würenlingen (Switzerland). For structural studies the double-axis multicounter diffractometer (DMC) was used [15]. The triple-axis spectrometer R5 served to measure the CEF excitations (a pyrolitic graphite monochromator, analyser and filter, with the analyser energy fixed at 15 meV, the modulus of the scattering vector Q in the range $1.4 \leqslant Q \leqslant 4.85$ Å^{-1} and the temperature in the range $12 \leqslant T \leqslant 150$ K). For zero-energy transfer the energy resolution was $\Delta E \simeq 1.2$ meV. The $NdGaO_3$ powder sample (15 g) was enclosed in a cylindrical V or Al container (12 mm diameter, 40 mm length) for the neutron diffraction or spectroscopy experiments, respectively.

3. Results

Our neutron diffraction study of $NdGaO_3$ shows that the nearest-neighbour oxygen ions around the Nd^{3+} site form considerably distorted octahedra (figure 1). The structural parameters obtained by a Rietveld refinement of the neutron powder diffraction patterns are listed in table 1. The space group of $NdGaO_3$ is P_{bn2_1} with C_2 point symmetry at the Nd site. Detailed results of the structure investigation will be described elsewhere [16].

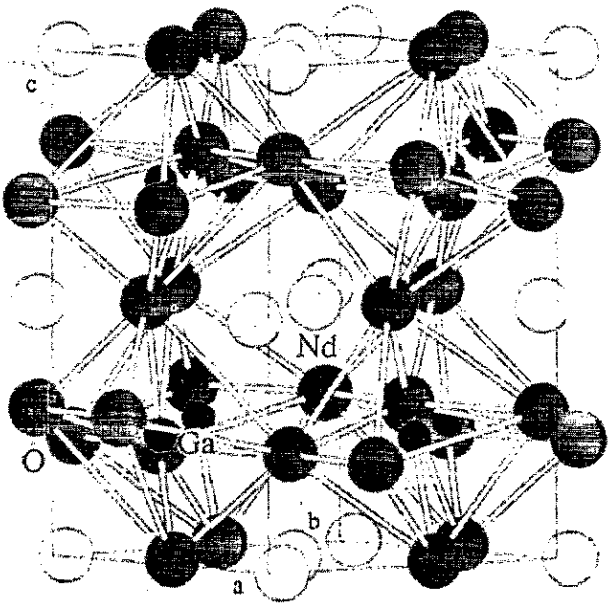

Figure 1. Crystal structure of $NdGaO_3$ showing the tilt of the oxygen octahedra.

Table 1. Structural parameters of $NdGaO_3$ at $T = 12$ K. Lattice parameters $a = 5.4243 \pm 0.0002$ Å, $b = 5.5014 \pm 0.0002$ Å, $c = 7.7016 \pm 0.0002$ Å; and atomic coordinates x, y, z.

	x	y	z
Nd	0.0102 ± 0.0004	0.0435 ± 0.0003	0.0000
Ga	0.505 ± 0.002	-0.004 ± 0.002	0.2562 ± 0.0008
O1	0.5826 ± 0.0004	-0.0189 ± 0.0004	0.0168 ± 0.0009
O2	0.288 ± 0.002	0.289 ± 0.002	0.217 ± 0.001
O3	0.296 ± 0.002	0.297 ± 0.002	0.805 ± 0.001

The INS spectra at $T = 12$ K exhibit four well-resolved inelastic curves at 11.4, 22.5, 52.7 and 68.0 meV (figure 2). It is well known that the intensities of CEF transitions decrease with increasing scattering vector due to the form factor, and their temperature dependences are governed by Boltzmann statistics, whereas phonon intensities usually increase with increasing scattering vector and their temperature dependences follow Bose statistics. Typical temperature dependences of the observed spectra are shown in figure 3. The phonon density of states of the non-magnetic reference compound $LaGaO_3$ measured

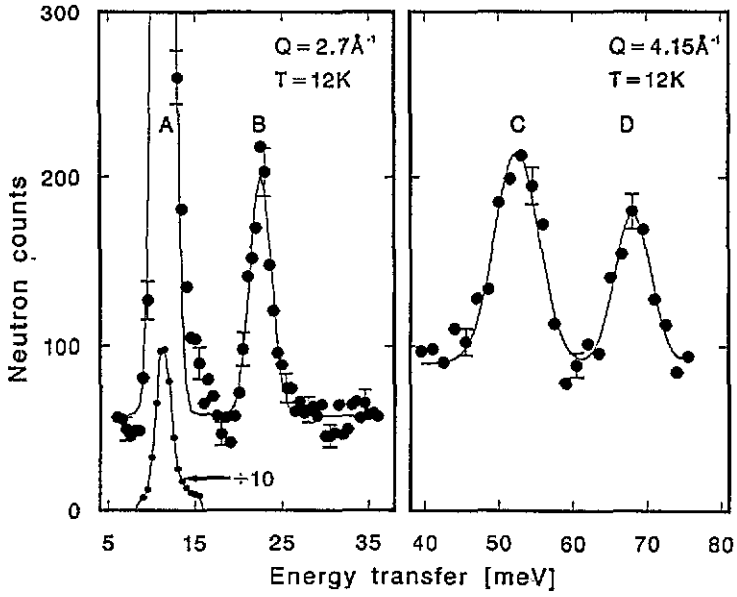

Figure 2. Energy spectra of neutrons scattered from $NdGaO_3$ at $T = 12$ *K*. The curves are the result of a least-squares fitting procedure in which the CEF transitions are described by single Gaussians.

at $T = 150$ K was found to exhibit a few broad inelastic lines with very small intensities, at least an order of magnitude smaller than the CEF transitions. Thus, we have clearly observed four inelastic peaks of magnetic origin.

We now consider the CEF transitions of figure 3 in detail. The peak intensities A, B, C and D decrease upon raising the temperature from 12 to 150 K. Therefore, we can interpret these four inelastic lines in terms of CEF transitions out of the ground state. The ten-fold degeneracy of the ground-state J multiplet $^4I_{9/2}$ of the Nd^{3+} ions is split by the CEF into five Kramers doublets. Thus, we have observed all possible excitations out of the ground state (marked with A, B, C, D) and thereby completely determined the energy level scheme of the Nd^{3+} ions in $NdGaO_3$, as shown in figure 4. The energy spectra taken at higher temperatures exhibit additional peaks (marked with E, F, G, H) which correspond to transitions out of excited CEF levels. From the temperature dependences and positions of these peaks we arrive at an assignment of CEF transitions as indicated in figures 3 and 4. Thus we have been able to unambiguously determine the energy-level scheme of Nd^{3+} in $NdGaO_3$ through the observation of all allowed ground-state as well as the majority of excited-state CEF transitions.

The magnetization measurements of the powder sample clearly show that there is no long-range magnetic ordering in the temperature range from 2 to 300 K. The magnetic susceptibility of single-crystalline $NdGaO_3$ turns out to be anisotropic (figure 5) with the c axis as the easy axis of magnetization. Above $T \simeq 150$ K the experimental data agree well with the Curie–Weiss law, from which an effective moment of $3.6\mu_B$ is obtained. This value is in good agreement with that expected for a Nd^{3+} free ion, $\mu_{eff}^{FI}(Nd^{3+}) = 3.62\mu_B$. Below 150 K a deviation from the Curie–Weiss law is expected due to CEF effects.

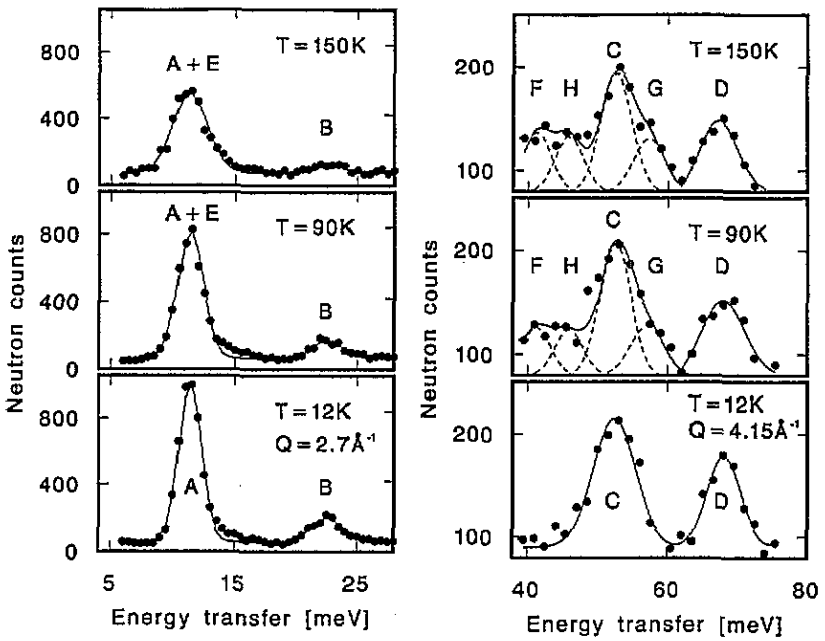

Figure 3. Energy spectra of neutrons scattered from $NdGaO_3$ for different temperatures. The curves are as in figure 2.

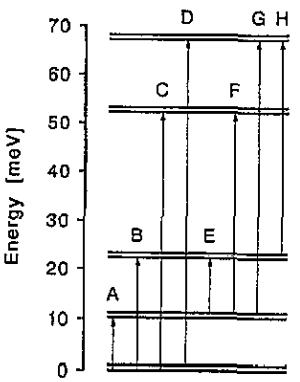

Figure 4. Energy level scheme of Nd^{3+} in $NdGaO_3$. The arrows denote the observed CEF transitions.

4. Analysis of results

Crystal-field calculations were carried out in the framework of single-particle crystal-field theory [17]. Without any external magnetic or exchange field, the corresponding Hamiltonian is as follows:

$$H_{\mathrm{CEF}} = \sum_{k,q,i} A_q^{(k)} C_q^{(k)}(i) \tag{1}$$

where $A_q^{(k)}$ is a crystal-field parameter and $C_q^{(k)}(i)$ a spherical tensor operator of rank k depending on the coordinates of the ith electron. The summation involving i is over all

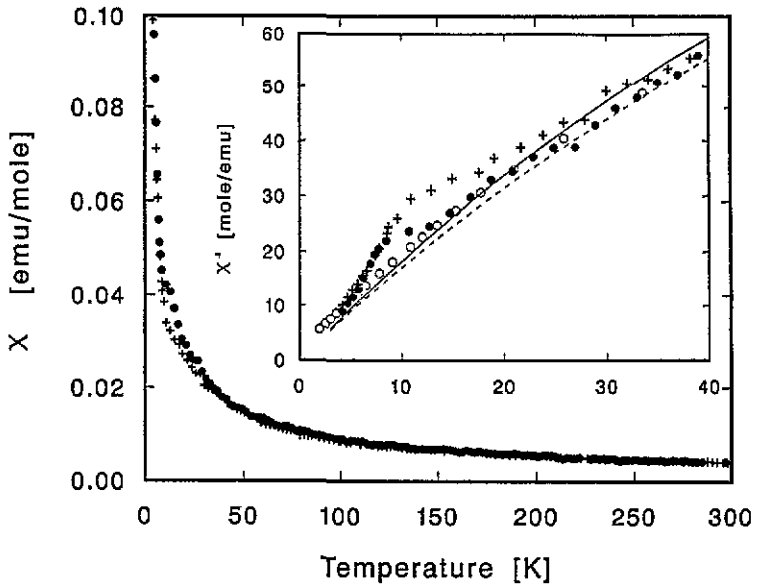

Figure 5. Temperature dependence of the magnetic susceptibility χ of single-crystal $NdGaO_3$ in an applied magnetic field of 0.004 T. The circles and crosses correspond to the components of the magnetic susceptibility parallel $\chi_{\parallel}^{-1}$ and perpendicular $\chi_{\perp}^{-1}$ to the c axis, respectively. Inset: comparison of observed and calculated (curves) inverse susceptibility data at low temperatures; open circles correspond to susceptibility data of the powder sample.

f electrons of the R ion. The values for k and q, for which the parameters $A_q^{(k)}$ are non-zero, depend on the site symmetry. Usually the CEF potential is treated as a perturbation of the ground-state J multiplet alone. However, for the compound examined here, the CEF splitting is about 70 meV and therefore comparable to the energy separation to the next J multiplet (approximately 250 meV), so these intermultiplet interactions cannot be neglected. A crystal-field formalism considering the ground-state J multiplet alone has been introduced by Stevens [18]:

$$H_{\mathrm{CEF}} = \sum_{n,m,\alpha} B_n^{m(\alpha)} O_n^m(i) \qquad \alpha = \mathrm{c}, \mathrm{s} \tag{2}$$

where $B_n^{m(\alpha)}$ is a CEF parameter and $O_n^m(i)$ an operator equivalent. $B_n^{m(\mathrm{c})}$ and $B_n^{m(\mathrm{s})}$ correspond to the real and imaginary part of the CEF parameters, respectively. The CEF parameters $A_q^{(k)}$ of equation (1) can easily be transformed into the CEF parameters $B_n^{m(\alpha)}$ of equation (2) by using normalizing coefficients [19]. Throughout this paper we will use the CEF parameters $B_n^{m(\alpha)}$ of the Stevens operator formalism.

The CEF potential of $NdGaO_3$ with C_2 symmetry at the Nd^{3+} site is characterized by 27 independent CEF parameters. Since we have only four observed lines and a few intensity ratios from our INS spectra, we cannot initially determine so many CEF parameters and we have to adopt some approximation. As repeatedly shown in the past [8–12] for several perovskite-type compounds, the CEF parameters $B_n^{m(\alpha)}$ for $n \geqslant 4$ may reasonably be determined by taking into account the geometry of the nearest-neighbouring coordination polyhedron:

$$B_n^{m(\alpha)} = (\gamma_n^{m(\alpha)}/\gamma_n^0) B_n^0 \qquad \alpha = \mathrm{c}, \mathrm{s}. \tag{3}$$

The coordination factors $\gamma_n^{m(\alpha)}$ ($\alpha = c, s$) are defined by Hutchings [20]. Again, $\gamma_n^{m(c)}$ and $\gamma_n^{m(s)}$ refer to the real and imaginary parts, respectively.

In order to cover all possible ratios B_4^0/B_2^0 and B_4^0/B_6^0 we introduce the parametrization [21]:

$$B_2^0 F_2 = W(1 - |y|) \qquad B_4^0 F_4 = Wxy \qquad B_6^0 F_6 = W(1 - |x|)y \tag{4}$$

with $F_2 = 2$, $F_4 = 60$, $F_6 = 2520$, $-1 \leqslant x \leqslant 1$ and $-1 \leqslant y \leqslant 1$. W is a scale factor. The off-diagonal CEF parameters were first fixed at their geometrical coordination values defined by equation (2). From a least-squares fit to the observed energy spectra we found two parameter sets ($x \simeq 0.2$, $y \simeq \pm 0.9$, $W \gtrless 0$) which gave reasonable agreement between the observed and calculated data. The two parameter sets differ only with respect to the sign of the CEF parameter B_2^0 which is known to determine the magnetic anisotropy. From the anisotropy of the observed single-crystal susceptibility measurements (see figure 5) we can immediately conclude that $B_2^0 < 0$, i.e. we retain the parameter set with $y < 0$ and $W < 0$. Except for the sign of B_2^0 the leading CEF parameters obtained in this way are close to those given for Nd^{3+} in the trigonal phase of $NdAlO_3$ [22]. We actually do not expect an agreement for the second-order CEF parameters, since they are governed by long-range electrostatic contributions. In a second step we have therefore allowed all the parameters $B_2^{m(\alpha)}$ to vary independently. We found that the $B_2^{1(\alpha)}$ parameters had only little influence on the overall behaviour of the CEF spectra, thus we assumed $B_2^{1(\alpha)} = 0$. The variation of $B_2^{2(\alpha)}$ turned out to improve the agreement between the observed and calculated intensities.

For $NdGaO_3$ there is a considerable spread of the radial extension of the coordination polyhedra around the Nd^{3+} ion. From the structural information listed in table 1 we derive the following ranges of the three nearest-neighbouring shells associated with the O^{2-}, Ga^{3+}, and Nd^{3+} ligand ions:

$$2.282 < R(Nd^{3+}\text{–}O^{2-}) < 3.431 \text{ Å}$$

$$3.152 < R(Nd^{3+}\text{–}Ga^{3+}) < 3.600 \text{ Å}$$

$$3.786 < R(Nd^{3+}\text{–}Nd^{3+}) < 3.941 \text{ Å}.$$

More distant coordination shells have interatomic distances larger than 4.33 Å. In the third step of our analysis we have therefore included the three nearest-neighbouring coordination polyhedra in the calculation of the geometry factors $\gamma_n^{m(\alpha)}$ by properly weighting with the nominal charges of the ligand ions. The resulting coordination factors are listed in table 2. The final CEF parameters turned out to be:

$$B_2^0 = (-0.1 \pm 0.1) \times 10^{-1} \text{ meV}$$
$$B_2^{2(c)} = -0.15 \pm 0.08 \text{ meV}$$
$$B_2^{2(s)} = 0.16 \pm 0.08 \text{ meV}$$
$$B_4^0 = (0.17 \pm 0.02) \times 10^{-2} \text{ meV}$$
$$B_6^0 = (0.16 \pm 0.01) \times 10^{-3} \text{ meV}.$$

The results of our analysis are summarized in table 3. In view of the underlying approximations the agreement between measured and calculated energy levels and normalized transition probabilities of the CEF states is rather good.

Table 2. Geometrical coordination factors for the Nd^{3+} site in $NdGaO_3$ calculated from the neutron diffraction data, as explained in the text.

n	m	$\gamma_n^{m(c)}$ (Å$^{-(n+1)}$)	$\gamma_n^{-m(s)}$ (Å$^{-(n+1)}$)
4	0	0.13×10^{-2}	
4	1	-0.57×10^{-2}	0.15×10^{-2}
4	2	0.32×10^{-2}	0.15×10^{-1}
4	3	-0.10×10^{-2}	0.62×10^{-2}
4	4	-0.30×10^{-2}	-0.18×10^{-1}
6	0	0.33×10^{-3}	
6	1	0.36×10^{-3}	0.29×10^{-3}
6	2	-0.67×10^{-3}	0.13×10^{-2}
6	3	-0.60×10^{-3}	-0.91×10^{-3}
6	4	0.84×10^{-2}	-0.24×10^{-3}
6	5	0.11×10^{-2}	0.27×10^{-2}
6	6	-0.13×10^{-2}	-0.30×10^{-3}

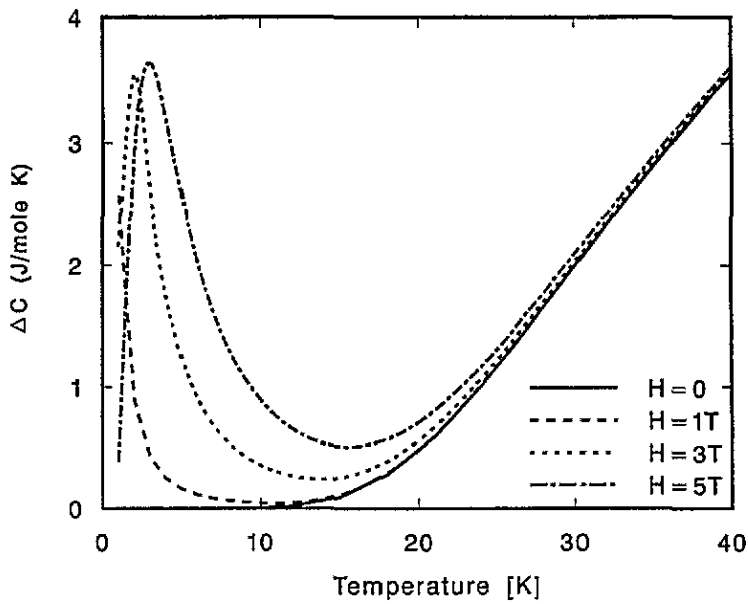

Figure 6. Schottky anomaly of the specific heat in magnetic fields up to 5 T, associated with the ground-state CEF splitting of Nd^{3+} in $NdGaO_3$, calculated on the basis of the present CEF parameters.

5. *Discussion and concluding remarks*

We have calculated the magnetic susceptibility on the basis of the CEF parameters derived in this paper. A nice agreement is obtained with the single-crystal data for $T > 25$ K as well as for the polycrystalline data (see figure 5). At present the discrepancy with the single-crystal data for $T < 25$ K is not understood.

Based on our CEF parameters we have calculated the Schottky anomaly of the specific heat in external magnetic fields, which essentially probes the wave functions of the ground doublet state of Nd^{3+} in $NdGaO_3$. The results are displayed in figure 6. However, to our

Table 3. Observed and calculated energy levels and normalized transition probabilities of the CEF states in $NdGaO_3$.

$\Gamma^{(i)}$	E_{obs} (meV)	E_{calc} (meV)	$\lvert\langle\Gamma^{(i)}\lvert J_p\rvert\Gamma^{(1)}\rangle\rvert^2_{obs}$	$\lvert\langle\Gamma^{(i)}\lvert J_p\rvert\Gamma^{(1)}\rangle\rvert^2_{calc}$	$\lvert\langle\Gamma^{(i)}\lvert J_p\rvert\Gamma^{(2)}\rangle\rvert^2_{obs}$	$\lvert\langle\Gamma^{(i)}\lvert J_p\rvert\Gamma^{(2)}\rangle\rvert^2_{cal}$
$\Gamma^{(1)}$	—	0	—	—		
$\Gamma^{(2)}$	11.4 ± 0.2	11.4	1.0	1.0	—	—
$\Gamma^{(3)}$	22.5 ± 0.4	22.6	0.2 ± 0.1	0.7	—	—
$\Gamma^{(4)}$	52.7 ± 1.0	52.4	0.9 ± 0.2	0.8	0.8 ± 0.4	0.5
$\Gamma^{(5)}$	68.0 ± 1.0	68.0	0.6 ± 0.2	0.5	0.8 ± 0.4	0.7

knowledge there is no information on the low-temperature specific heat of $NdGaO_3$ in the current literature.

In conclusion, we have presented a study of crystalline-electric-field and magnetic properties of $NdGaO_3$ by means of INS and magnetic susceptibility measurements. A set of CEF parameters has been derived in terms of single-particle crystal-field theory based on geometrical coordinations associated with the C_2 site symmetry of Nd^{3+} and J-mixing between all multiplets of the ^4I term, which adequately explains the majority of magnetic and crystal-field properties of $NdGaO_3$. Our results may easily be used to extrapolate the CEF interaction to other compounds having related structures. At present we are involved in further studies of the CEF interaction in $RGaO_3$ and $RNiO_3$ compounds, in order to understand the nature of the electronic localization in the nickelates.

Acknowledgments

One of the authors (AP) is grateful to the Swiss National Science Foundation for financial support of a post-doctoral position. The authors would like to thank Drs A Schilling and S Verkhovskii for performing magnetic susceptibility measurements. The help of Dr M Berkowski with crystal growth and partial support from Thomson-CSF and from the Swiss National Science Foundation (Project No 2120-031.199.91) for crystal growth are appreciated.

References

[1] Bednorz J G and Müller K A 1986 *Z. Phys.* B **64** 189
[2] Maekava S, Ohta Y and Tohyama T 1992 *Springer Series in Solid-State Science* vol 106 (Berlin: Springer) p 29
[3] García-Muñoz J L, Rodríges-Carvajal J, Lacorre P and Torrance J B 1992 *Phys. Rev.* B **46** 4414
[4] García-Muñoz J L, Rodríges-Carvajal J and Lacorre P 1992 *Europhys. Lett.* **20** 241
[5] Medarde M, Fontaine A, García-Muñoz J L, Rodríges-Carvajal J, de Santis M, Sacchi M, Rossi G and Lacorre P 1992 *Phys. Rev.* B **46** 14975
[6] Marezio M, Dernicz P D and Remeika J P 1972 *J. Solid State Chem.* **4** 11
[7] Cohen E, Riseberg L A, Nordland W A, Burbank R D, Sherwood R C and Van Uitert L G 1969 *Phys. Rev.* **186** 476
[8] Furrer A, Brüesch P and Unternährer P 1988 *Phys. Rev.* B **38** 4616
[9] Podlesnyak A, Kozhevnikov V, Mirmelstein A, Allenspach P, Mesot J, Staub U, Furrer A, Osborn R, Bennington S M and Taylor A D 1991 *Physica* C **175** 587
[10] Mirmelstein A, Podlesnyak A, Voronin V, Lebedev S, Goshchitskii B, Allenspach P, Mesot J, Staub U, Guillaume M, Fischer P and Furrer A 1992 *Physica* C **200** 337
[11] Mesot J, Allenspach P, Staub U, Furrer A, Mutka H, Osborn R and Taylor A 1993 *Phys. Rev.* B **47** 6027
[12] Mesot J, Allenspach P, Staub U, Furrer A and Mutka H 1993 *Phys. Rev. Lett.* **70** 865
[13] Sandstrom R L, Giess E A, Gallagher W J, Segmüller A, Cooper E I, Chisholm M F, Gupta A, Shinde S and Laibowitz R B 1988 *Appl. Phys. Lett.* **53** 1874
[14] Schilling A 1992 *Dissertation* ETH Zürich, No 9645, p 102
[15] Schefer J, Fischer P, Heer H, Isacson A, Koch M and Thut R 1990 *Nucl. Instrum. Methods* A **288** 477
[16] Marti W, Fischer P, Altorfer F, Scheel H J and Tadin M 1993 *J. Phys.: Condens. Matter* submitted
[17] Wybourne B G 1965 *Spectroscopic Properties of Rare Earths* (New York: Interscience)
[18] Stevens K W H 1952 *Proc. Phys. Soc.* A **65** 209
[19] Dieke G H 1965 *Spectra and Energy Levels of Rare Earth Ions in Crystals* (New York: Interscience)
[20] Hutchings M T 1964 *Solid State Physics* vol 16, ed F Seitz and D Turnbull (New York: Academic) p 227
[21] Lea K R, Leask M J M and Wolf W P 1962 *J. Phys. Chem. Solids* **23** 1381
[22] Finkman E, Cohen E and Van Uitert L G 1973 *Phys. Rev.* B **7** 2899